THE ONSET OF SEPARATION IN NEUTRAL, TURBULENT FLOW OVER HILLS

NIGEL WOOD
Meteorological Office, Bracknell, Berkshire, RG12 2SZ, UK

(Received in final form 3 May, 1995)

Abstract. The onset of separation in turbulent, neutrally stratified, boundary-layer flow over hills is considered. Since the flows are fully turbulent, the occurrence of intermittent separation, in the sense of any reversal of near surface flow, will depend strongly on the detailed structure and behaviour of the turbulent eddies. Very little is known about such intermittent separation and the phenomenon cannot be studied with numerical models employing standard turbulence closures; eddy-resolving models are required. Therefore, here, as elsewhere in the literature, the arguably less physically significant process of mean flow separation is studied. Numerical simulations of flow over idealised two- and three-dimensional hills are examined in detail to determine the lowest slope, θ_{crit}, for which the mean flow separates.

Previous work has identified this critical slope as that required to produce a zero surface stress somewhere over the hill. This criterion, when a mixing-length turbulence closure is applied, reduces to requiring the near-surface vertical velocity shear to vanish at some point on the hill's surface. By applying results from a recent linear analysis for the flow perturbations to this condition, a new expression for θ_{crit} is obtained. The expression is approximate but its relative simplicity makes it practically applicable without the need for use of a computer or for detailed mapping of the hill. The approach suggested differs from previous ones in that it applies linear results to a non-linear expression for the surface stress. In the past, a linear expression for the surface stress has been used. The proposed expression for θ_{crit} leads to critical angles that are about twice previous predictions. It is shown that the present expression gives good agreement with the numerical results presented here, as well as with other numerical and experimental results. It is also consistent with atmospheric observations.

1. Introduction

Linear theory (e.g. Jackson and Hunt, 1975; Belcher *et al.*, 1993) shows that the flow perturbations induced by the presence of a low hill are dominated by inviscid dynamics. This predicts that the effect of a hill on the flow past it, is to induce a negative pressure perturbation at the crest of the hill so that the flow is accelerated up the upstream slope. There is also a positive pressure perturbation downstream of the hill which decelerates the flow on the downstream slope. As discussed by Lighthill (1989), this adverse pressure gradient leads to the production of near-surface vorticity of opposite sense to the boundary-layer vorticity. At low slopes, the rate of production of this vorticity is small and it is annihilated by cross-diffusion with the boundary-layer vorticity without having much impact on the flow. However, for such slopes the rate of production of this vorticity is proportional to the slope, and as this increases, so too does the adverse pressure

Boundary-Layer Meteorology **76:** 137–164, 1995.

gradient. Eventually the vorticity that this pressure gradient creates dominates; and in two dimensions, a reversed flow occurs near the surface. Where this reversed flow meets the downslope flow, there is a region of large convergence leading to a component of velocity normal to the surface. Thus, the near-surface streamline that approaches this point is lifted away from the surface. In a Lagrangian sense, Van Dommelen and Cowley (1990) view this process as the formation of a singularity in the continuity equation. The converging flow compresses the fluid element in a direction tangential to the surface, resulting in the ejection of fluid away from the boundary.

This process of streamlines or fluid elements migrating away from the near surface is called separation. In the above discussion, only laminar flows have been considered. If the flow is turbulent, its mean properties are governed by the ensemble-averaged Navier–Stokes equations. Neglecting the effects of molecular viscosity, i.e. assuming very high Reynolds number flow, and applying an eddy-viscosity closure for the Reynolds stresses, the resulting equations are very similar in form to those for laminar flow, except now viscosity is in general dependent on the flow itself. This suggests that apart from the influence of the spatially varying viscosity, the qualitative picture given above should still be valid for the turbulent flows discussed here.

Whilst non-linear effects in the mean flow may be present prior to separation, they become dominant after it has occurred. The onset of separation causes a significant change in the mean streamline patterns and in other flow characteristics such as the surface drag (Wood and Mason, 1993). Also, for turbulent boundary layers, when the flow does not separate, most of the mean flow vorticity is confined relatively close to the surface. Thus the structure of the inner region (where the turbulence is in local equilibrium) has little effect on the outer region (where the turbulence is governed by rapid distortion dynamics and the flow perturbations are approximately inviscid). This is in contrast to laminar boundary layers, as discussed by Hunt *et al.* (1988). However, once the flow separates, the surface vorticity can be transported far from the surface, possibly leading to an elevated shear layer. This will then influence the flow in the outer region.

It is clearly very important to know whether the flow is separated or not. Even to diagnose this is not straightforward. This will be discussed in the next section where three different types of flow visualization will be used to estimate the value of the critical slope for separation from numerical model simulations.

Attention is then turned to trying to predict this critical slope, the primary aim being to obtain a simple, approximate estimate of θ_{crit} that can be applied in practical situations to a particular hill without the need for use of a computer and without recourse to detailed mapping of the hill. Such an estimate should be useful, for example, in simple dispersion or pollution models to indicate where possible trapping of a pollutant in the lee of a hill may occur. It might also be useful in predicting when the results of linear predictions of the flow field are likely to be applicable.

In Section 3 the case of a two-dimensional sinusoidally shaped hill is used to develop a relatively simple formula for θ_{crit} which, it is demonstrated empirically in Section 4, can be used successfully to indicate the onset or not of separation for more realistically shaped hills.

The philosophy of this approach is the same as has proved successful in estimating the maximum flow speed-up over hills. Mason (1986) found good agreement between the observed maximum fractional speed-up above Nyland Hill and an estimate based on simple, linear scaling arguments. Belcher *et al.* (1993) also obtain good agreement between observed profiles of fractional speed-up above Askervein and the predictions of linear theory applied to simple, idealised hill shapes. These and other similar results have led to the adoption of very simple, general estimates of the maximum fractional speed-up (e.g. Taylor and Lee, 1984) which have been incorporated into building codes (e.g. BRE, 1989). Of course, as with any approximate formula which is verified empirically, caution must be taken when applying such results in practice, as in extreme circumstances they may prove to be inaccurate. However, when applied carefully, such estimates can be useful.

2. Diagnosing the Onset and Nature of Separation

Wood and Mason (1993) discussed three different sets of simulations of flow over hills. In this section, the flow fields from these series of simulations will be discussed and the slope at which separation first occurs will be estimated.

The first set simulates flow over two-dimensional hills, or ridges. The width of the hill (λ) is the same as the width of the numerical domain (1000 m). So, by virtue of the periodic lateral boundary conditions, this series simulates flow over an infinite corrugated surface. The hills are referred to as "two-dimensional packed" hills. The second set is similar to the first but now the hills are three-dimensional having a circular horizontal cross-section. The diameter of the hills equals the domain width in both horizontal directions so the periodicity makes these hills appear like infinite, upturned egg boxes and are called "three-dimensional packed". The third set keeps the same hill shape and hill diameter (1000 m) but the numerical domain is 4000 m by 4000 m. The resulting distance between neighbouring hills is sufficient that the hills are effectively isolated hills and are referred to as "three-dimensional isolated". The surface of all the hills, $Z_s(x, y)$, is given by:

$$Z_s(x,y) = \begin{cases} h(\cos(\pi\sqrt{(x/\lambda)^2 + (y/\lambda)^2}))^2 & \text{for } x^2 + y^2 \leq \lambda^2/4 \\ 0 & \text{for } x^2 + y^2 > \lambda^2/4 \end{cases}$$

with $y \equiv 0$ for the two-dimensional case.

All runs have 40 grid points in the vertical, stretched logarithmically near the surface with the lowest internal grid point at 0.1 m above the local surface. In the horizontal, the two-dimensional runs have 20 uniformly spaced grid points and the

three-dimensional packed runs have 20 × 20 grid points. The three-dimensional isolated hills have 40 × 40 grid points in the horizontal with the grid spacing in the region of the hills similar to the other two cases but with the grid spacing stretched away from the hill.

For all cases considered here, the driving force is a 10 m s^{-1} geostrophic wind (in a direction perpendicular to the ridges); a Coriolis parameter of 10^{-4} s^{-1} is used; and a surface roughness length Z_0 = 0.1 m is chosen. All simulations are run for 3000 s after being initialised with a steady, one-dimensional, planetary boundary-layer profile, derived from a steady-state version of the same model equations. Within each set of runs, the simulations differ from each other only in the height of hill modelled. The height is varied from 50 to 300 m in 50 m steps with a further run with a hill height of 10 m. This represents a change in the tangent of the maximum slope of the hills from θ = 0.03 to 0.94, i.e., a change in slope from less than 2 to 43°. (In what follows, θ and θ_{crit} strictly represent the gradient of the hill, i.e., the tangent of the slope of the hill but, following convention, they will generally be referred to as slopes.)

The numerical model solves the Boussinesq approximation to the ensemble-averaged Navier–Stokes equations for the three components of velocity as well as the mass continuity equation and an equation for the turbulent kinetic energy (for use in the $1\frac{1}{2}$-order turbulence closure). The equations are solved in a terrain-following co-ordinate system without transformation of the Cartesian velocity components (e.g. Clark, 1977). Further details of the model and numerical schemes employed can be found in Wood (1992) and Wood and Mason (1993).

2.1. TWO-DIMENSIONAL HILLS

In two dimensions, the diagnosis of separation is relatively straightforward. In this case, a streamfunction may be defined and evaluated numerically. Since the no-slip condition is imposed, the surface is always a streamline but this streamline can split with a section departing from the surface to enter the interior of the fluid. Such an occurrence indicates separation.

The streamlines evaluated from the model results in two dimensions are plotted for hill heights h = 100, 150 and 200 m in Figures 1 to 3. For h = 100 m the surface streamline does not separate though a marked thickening of the boundary layer in the lee of the hill is evident. For h = 150 m, however, the surface streamline clearly separates close to half way down the lee slope and reattaches about a third of the way up the up-slope of the next hill downstream. As the height of the hill increases, the point of separation moves slowly upstream towards the crest of the hill. The point of reattachment moves downstream towards the crest of the downstream hill. For the steepest hill simulated, h = 300 m (not shown here), over half of the depth of the valley (peak to trough) is filled with recirculating fluid. These results are consistent with the findings of Newley (1985) for the same shaped hills, that the point of separation is close to where the surface pressure perturbation

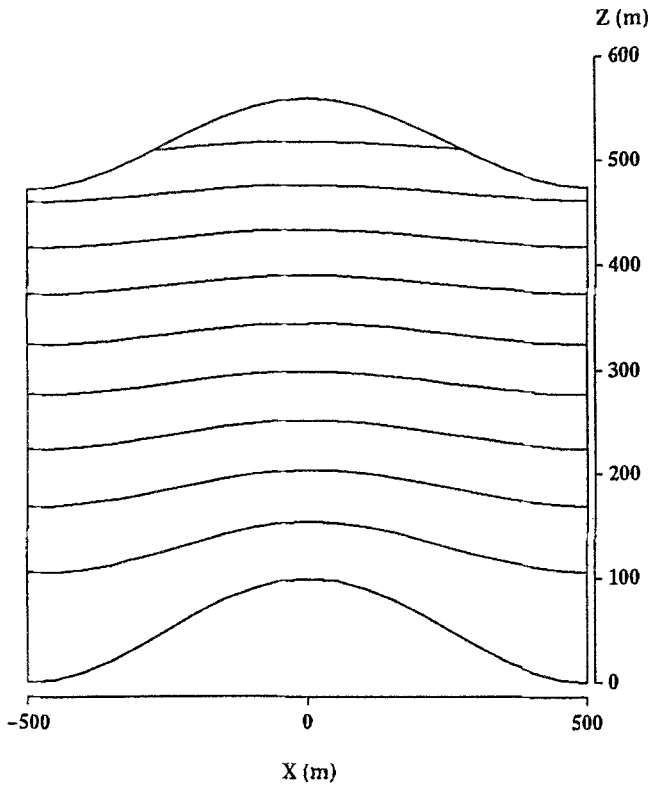

Fig. 1. Streamlines from the numerical simulation of flow over a two-dimensional, cosine-squared shaped hill. The hill has wavelength, λ = 1000 m and height 100 m corresponding to $\theta \simeq 17^{\circ}$.

reaches zero and that reattachment occurs close to the maximum surface pressure perturbation.

From Figures 1 to 3, it may be concluded that the flow does not separate until $h > 100$ m. However this is not the case. Figure 4 shows a portion of the horizontal profile of the component of surface stress parallel to the surface, normalised by its value in the absence of the hill, for h = 100 m. (The crest of the hill is at $X/\lambda = 0$ and the trough is at $X/\lambda = 0.5$.) It is seen that the stress reverses sign in the region indicated by the arrow. This region is centred about 400 m downstream of the crest of the hill. This indicates convergence of mass parallel to the surface which, due to the imposition of incompressibility and zero mass flux through the lower boundary, requires a non-zero normal velocity component and therefore separation of the surface streamline. This is not evident in Figure 1 because the region of reversed flow is very small in both its horizontal and vertical extent and is beyond the resolution of the plotting routine. Thus, it is concluded that the present two-dimensional simulations of flow over a sinusoidally shaped ridge with $\lambda/Z_0 = 10^4$, just separate at h = 100 m, for which $\theta = 0.31$ and $A/S_h = 0.1$ (where A is the

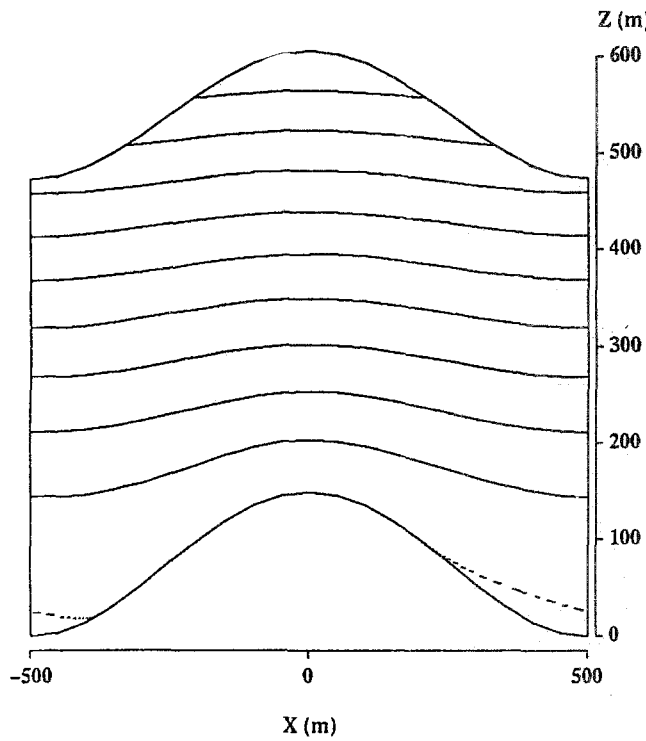

Fig. 2. As for Figure 1 but the hill now has height 150 m and $\theta \simeq 25°$. The dotted line indicates the zero value streamline and hence separation.

frontal, or silhouette area of the hill and S_h is its base area). This result will be discussed in relation to other such results in Section 4 below.

2.2. THREE-DIMENSIONAL HILLS

Since a streamfunction cannot be defined in three dimensions, the above procedure to determine whether or not the flow is separated, cannot be applied. However, if the flow is steady (which is approximately true for the cases presented here), the streamline pattern is the same as the pathline pattern and the streamlines may be evaluated by tracing the path of a particle released into the flow. The flow is separated if any such particle that is released arbitrarily close to the surface moves a finite distance from the surface. Conversely, if all the particles remain within the same order of distance from the surface as the height at which they are released, the flow is everywhere attached or unseparated. This, though, is an arduous and time-consuming task to perform in practice. Further, due to numerical limitations, particles cannot be released arbitrarily close to the surface and from a practical point of view, with a finite height of release, it is not obvious how to define what

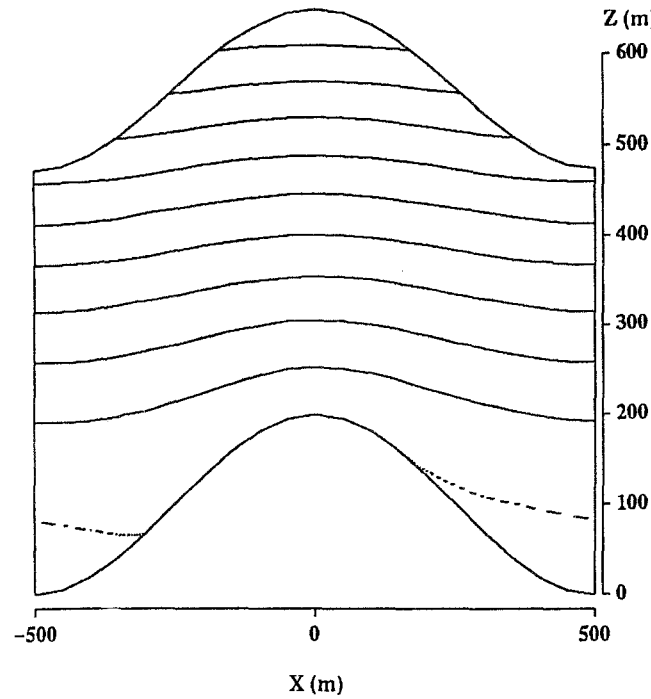

Fig. 3. As for Figure 1 but the hill has height 200 m and $\theta \simeq 32°$.

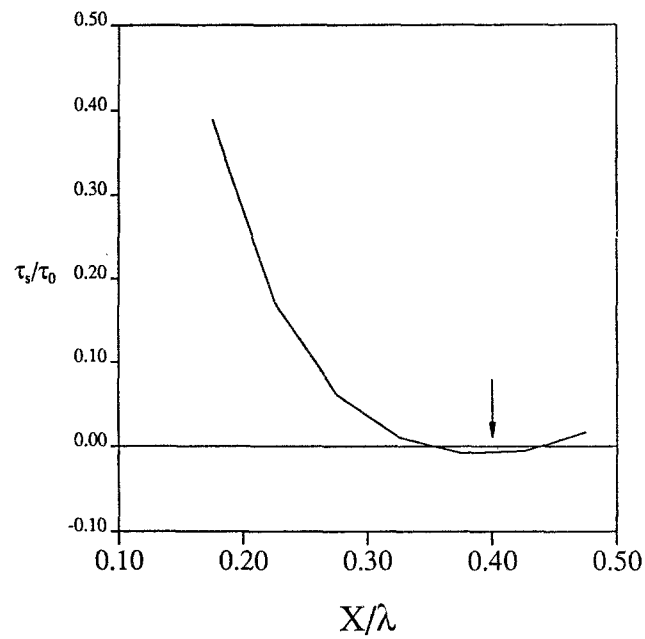

Fig. 4. A portion of the horizontal profile of the surface stress component parallel to the surface, normalised by the undisturbed value of stress, for a hill height h = 100 m. (The crest of the hill is at $X/\lambda = 0$ and the trough is at $X/\lambda = 0.5$.)

height such particles have to reach before separation may be deemed to have occurred. Therefore here a different technique, detailed below, is used to determine separation. As well as this, trajectories of two particles are used to visualise part of the flow.

As discussed above in relation to two-dimensional flows, separation occurs as a result of strong convergence induced by the perturbation pressure force due to the hill. This is true also in three dimensions, though the convergence may then be due to the lateral component of velocity. Hence, one of the easier ways of looking for evidence of separation is to consider the surface stress patterns. These are plots of a collection of two-dimensional trajectories using the two horizontal components of the surface tangential stress as the "velocity" field. The method of calculating these and also for calculating the trajectories of the fluid particles, plotted here in perspective, is essentially the same as that described in Mason and Sykes (1979a) and uses a fourth-order Kutta–Merson integration technique.

A singularity in the surface stress is any point or line at which the magnitude of the surface tangential stress vector vanishes. Hunt *et al.* (1978) note that such a singularity usually indicates a point or line at which the flow is either separating from or reattaching to the surface. The singularities may be classified as either nodes or saddle points of separation or attachment. There are methods for determining the classification of the singularity from the local surface stress field (see Hunt *et al.*, 1978). However, the present numerical mesh is not fine enough to resolve the behaviour of the stress near a singularity with sufficient accuracy to follow this procedure. Hence, in what follows the singularities have been classified visually from the pattern of the stress "streamlines". A saddle point has only two shear stress lines passing through it. On one of these, the stress vectors either side of the singularity will be directed towards the singularity whilst on the other, the vectors either side will be directed away from it. Thus on each line the vector changes its direction at the singularity. A node has an infinite number of stress lines meeting at it. If it is a node of separation, the stress vectors will all be directed towards the node. If it is a node of attachment, they will all be directed away from it.

It is important to note that it is generally assumed that a singularity point is a necessary condition for the presence of separation. However, Mason and Sykes (1979a) found that in their numerical simulations of laminar flow over hills, separation did, in certain circumstances, occur with no singularity in the stress field. The cause of this phenomenon is not clear but appears to be related to asymmetry in the forcing of the flow (in Mason and Sykes' case, this was the rotation of the frame of reference).

Figures 5 to 7 show surface stress patterns and corresponding perspective plots of two trajectories for the packed three-dimensional hills with h = 100, 150 and 200 m. In each trajectory plot one particle is released from the crest of the hill at a height of about 0.65 m above the surface and, relative to the stress patterns, the other particle is released from the lower left-hand corner at the same height above the surface.

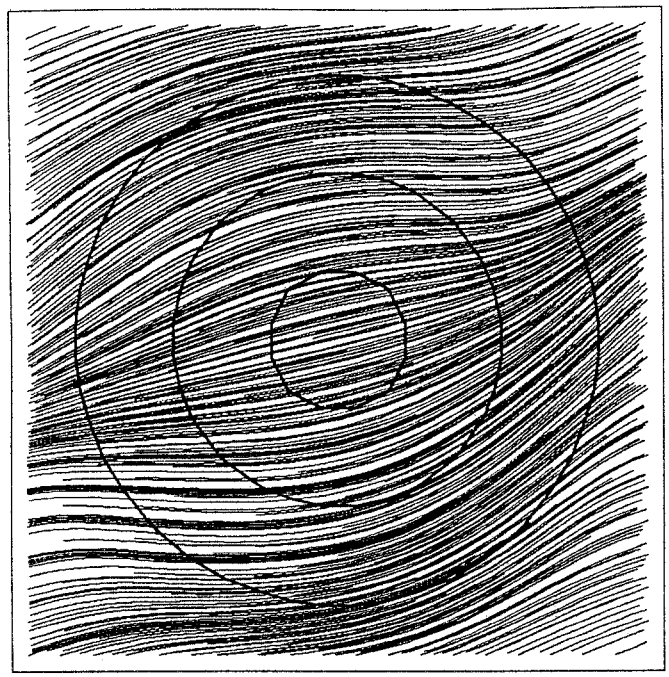

Fig. 5a. Surface stress patterns (streamlines evaluated using the horizontal components of the surface stress) from the numerical simulation of flow over a packed three-dimensional hill. The diameter of the hill is 1000 m and its height h = 100 m giving $\theta \simeq 17°$. The circular lines are contours of the hill's surface at surface heights $0.9h$, $0.5h$ and $0.1h$.

For h = 100, the stress "streamlines" are deflected by the hill and converge in its lee. However, the convergence is not very strong and there is no evidence of a singularity forming near the surface. The trajectory from the crest rises to a maximum height above the surface of 2.9 m, the other trajectory remaining much nearer the surface. This lifting of the trajectory is not dramatic but is evidence of the thickening of the boundary layer in the lee of the hill. For h = 150 m, the convergence has become considerably greater but there is still no singularity in the stress pattern. However, the trajectory from the crest reaches a height of 6.9 m above the surface in the lee of the hill. There is also the appearance of a kink in the other trajectory followed by a slight lifting. However, there is still no clear evidence of separation such as Mason and Sykes found for their case with no stress singularity. By h = 200 m, there are clearly two singularity points just upstream of the base of the hill. One is a saddle point of separation upstream of, but close to, a nodal point of attachment. Due to the periodicity of the flow, the separation point is seen to be at the end of the convergence line. As the hill height increases further, there is no change in the topology of the flow. The points of separation and attachment become more distinct and the convergence line becomes a sharper feature. For $h \geq 200$ m, plots of the trajectories (only that for h = 200 m is shown

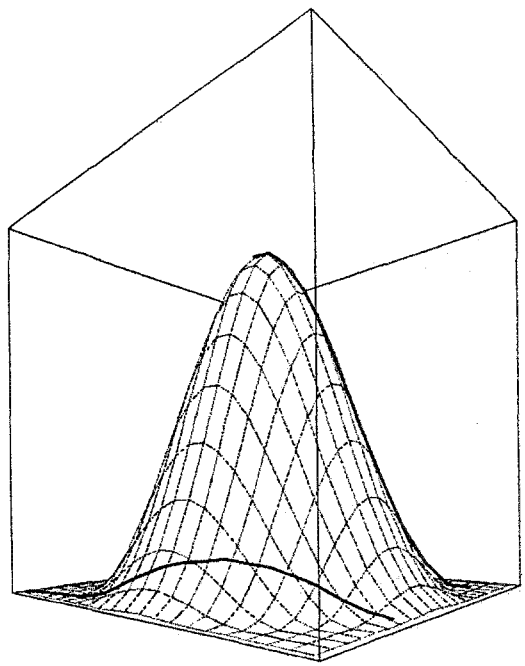

Fig. 5b. Perspective plot of the trajectories of two particles released into the flow field of the run shown in Figure 4a. The view of the hill is from a slightly elevated position and is nearly from the south-easterly direction (where the positive y-axis is in the northerly direction and the positive x-axis is in the Easterly direction). The two particles are released from a height of about 0.65m above the surface, one from the South-Westerly corner of the domain and the other from the crest of the hill. In the plot the heights of the trajectory and the hill's surface are scaled by $1.1h$. In these units the top of the box plotted is at a height of 1.

here) all show a similar picture and give a clear indication of the strong convergence and upslope flow followed by separation from the surface.

These diagrams suggest that the flow is still attached at $h = 150$ m but separated for $h = 200$ m (for which $\theta = 0.63$ and $A/S_h = 0.1$).

Figures 8 to 10 show the surface stress patterns and trajectory plots for the isolated hills with $h = 150$, 200 and 250 m. The release points and heights correspond approximately to those for the packed hills. For convenience, only the central portion is presented of the full 4 km $\times$ 4 km domain, which is similar in dimensions to the domain presented for the packed hills.

For $h = 150$ m, the surface stress patterns for the isolated case are in essence very similar to those for the packed case at the same hill height. However, in the packed case, the downstream hill causes a region of large pressure on its upstream slope, which strongly diverts the flow round the hill in question. This leads to a highly asymmetric velocity field in the lee of the hill and a consequent enhancement of the convergence compared with that seen in the isolated case.

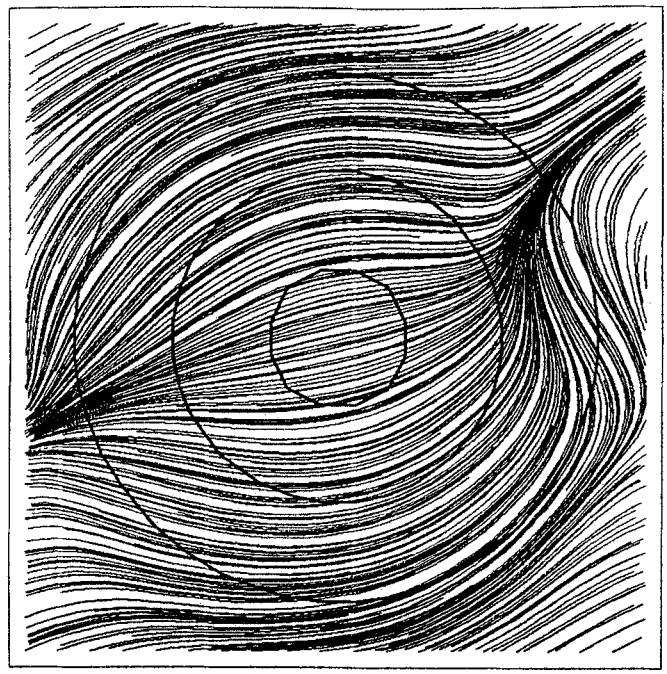

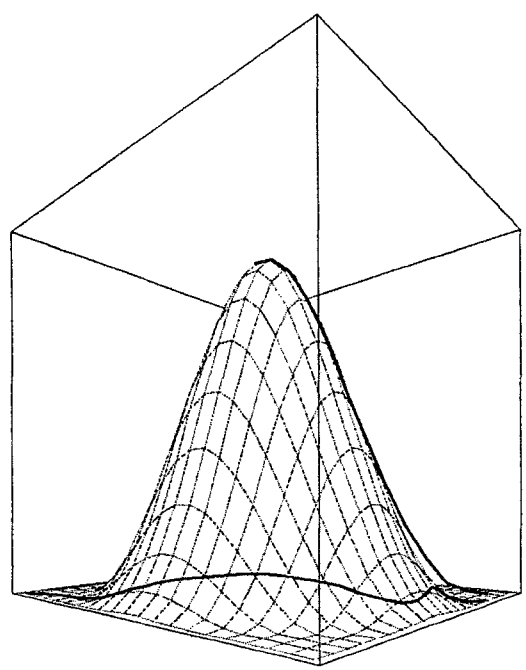

Fig. 6a,b. As for Figures 5a and 5b but for a hill height $h = 150$ m corresponding to $\theta \simeq 25°$.

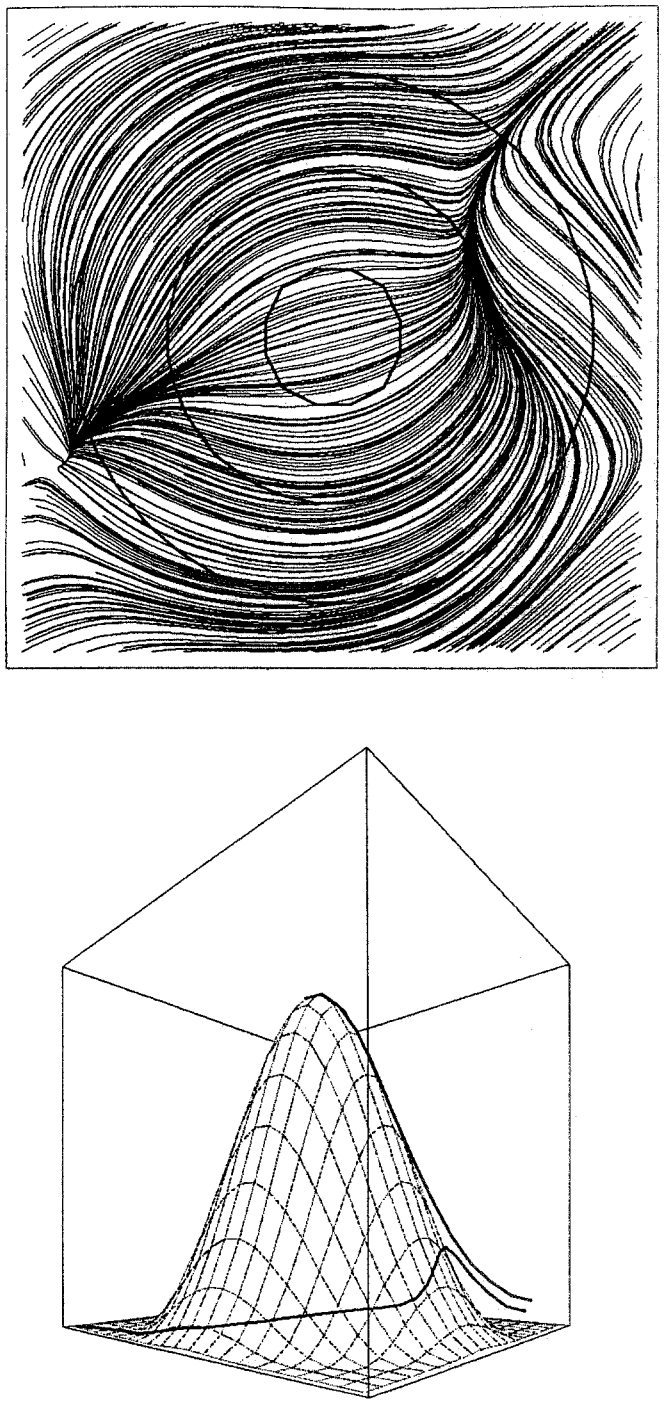

Fig. 7a,b. As for Figures 5a and 5b but for a hill height $h = 200$ m corresponding to $\theta \simeq 32°$.

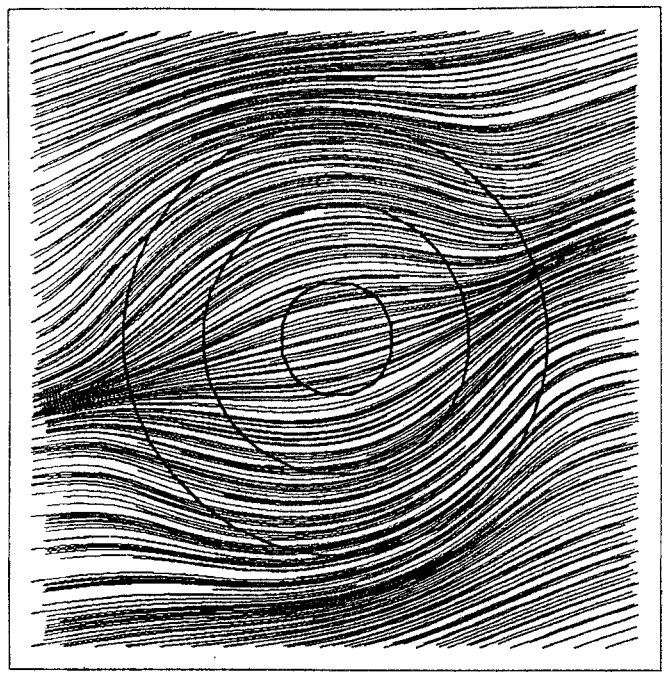

Fig. 8a. Surface stress patterns from the numerical simulation of flow over an isolated three-dimensional hill. The hill has a diameter of 1000 m and hill height h = 150 m, corresponding to $\theta \simeq 25°$. Only the central portion of the domain is shown so that the horizontal extent of this plot corresponds approximately with the same area, relative to the hill, as presented in Figures 5a–7a. Again the circular lines are contours of the hill's surface at surface heights $0.9h$, $0.5h$ and $0.1h$.

A significant change in the surface stress patterns is seen between h = 150 m and h = 200 m. For the latter there is clearly flow separation with upslope flow in the lee of the hill. The nature of the separation is different to that of the packed case. There is a well defined nodal point of separation, a nodal point of attachment and evidence of two saddle points connecting these nodes. Upstream, near the base of the hill, there is a region of strong convergence.

Despite the evidence in Figures 8a to 10a suggesting that there is separation at h = 200 m with reversed upslope flow in the lee of the hill, there is only minimal evidence from the trajectories. The trajectories shown are typical of many others that have been considered and only lift slightly from the surface reaching a height of 7.1 m (compared with 23.6 m for the packed case). When released as close to the surface as the vertical resolution will allow (0.1 m), the particle moves up the downslope but due to the limitations of the trajectory routine, hits the surface. Particles released much higher than this show the same basic behaviour as those presented here. This indicates that the separation is a very small feature in terms of its vertical extent. Even for h = 250 and 300 m (not shown here), the trajectories only reach maximum heights of 13.1 and 36.1 m respectively, and at this height,

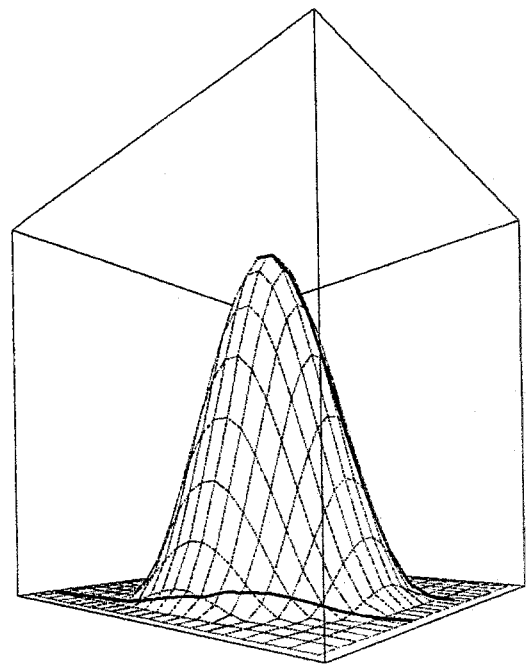

Fig. 8b. Perspective plot of the trajectories of two particles released into the flow field of the run shown in Figure 8a. As in Figure 8a, only the central portion of the domain is shown so that the horizontal extent of the plot corresponds approximately with the same area, relative to the hill, as presented in Figure 5b. The particles are released from the same height and similar positions, relative to the hill, as in Figure 5b.

there is no sign of the reversed flow. The more localised nature of the separation and hence the greater horizontal shear in the isolated case is clear from the trajectories in these last two cases in which the rate of change of the particles' direction is much greater than for the packed cases.

Again these diagrams suggest that the flow is still attached at h = 150 m but separated for h = 200 m (for which $\theta = 0.63$ and $A/S_h = 0.1$).

In the next section, a formula giving θ_{crit} as a function of the ratio of the horizontal length scale of the hill to its surface roughness, λ/Z_0, is proposed. Its predictions for θ_{crit} will be compared with the above results in Section 4.

3. A Linearised Estimate of the Critical Slope

For very high Reynolds' number flows, such as those considered here, it is generally accepted (see for example Mason and King (1984)) that the onset of separation depends on the peak slope exceeding some critical value, θ_{crit} say, which will depend on the roughness length and the exact shape of the hill. The dependence on the surface roughness length, Z_0, arises because, as noted by Britter *et al.* (1981), when

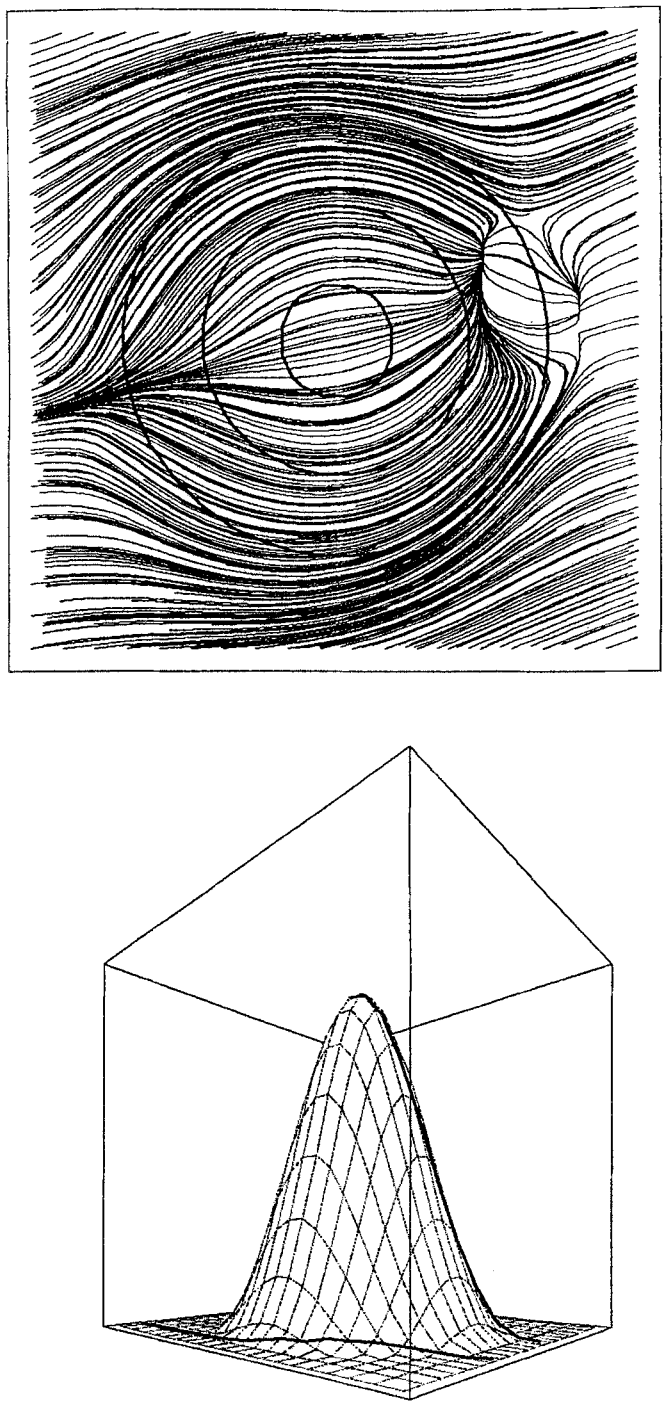

Fig. 9a,b. As for Figures 8a and 8b but for a hill height h = 200 m corresponding to $\theta \simeq 32°$.

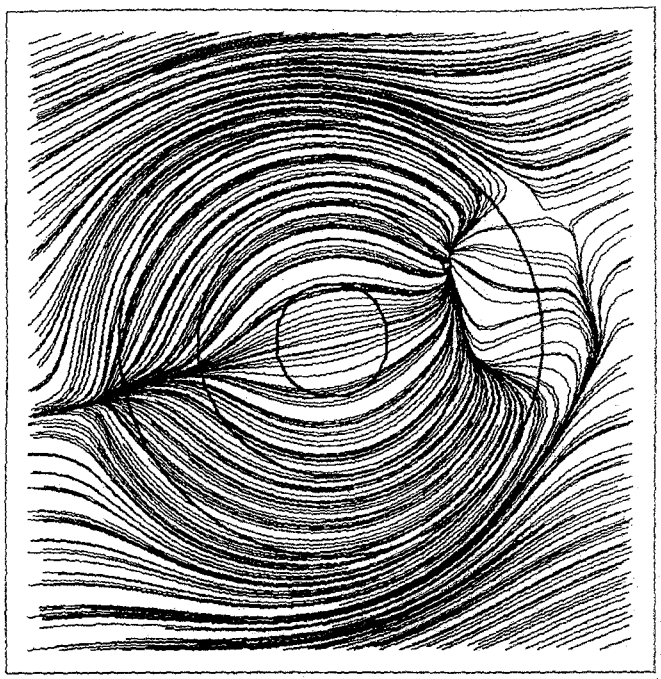

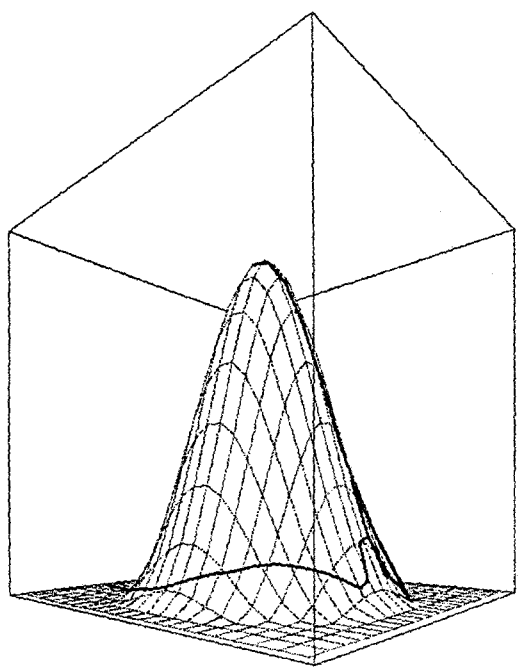

Fig. 10a,b. As for Figures 8a and 8b but for a *hill* height $h = 250$ m corresponding to $\theta \simeq 38^{\circ}$.

Z_0 decreases, for a given slope, the near-surface flow speed increases, enabling the boundary layer to support a larger adverse pressure gradient before it separates. Conversely, as Z_0 increases, the near-surface flow is reduced and the shear in the mean flow is increased and, in the absence of other factors, these make separation more likely. However, diffusion will also increase, inhibiting separation. It is clear that the exact dependence of θ_{crit} on Z_0 is not simple.

The analytical work of Hunt *et al.* (1988a) and Belcher *et al.* (1993), as well as the observational and modelling comparisons of Mason and King (1985) suggest that linear analysis provides good predictions of the mean flow characteristics up to slopes for which the flow is nearly separated. Further, if consideration is restricted to flow upstream of the point of separation, the linear results may still provide reasonable agreement with observations of the mean flow. Thus, whilst non-linear effects become very important close to separation, it may be possible to obtain an approximate value for θ_{crit} by extrapolating the linear results to see where they predict separation.

This is the method that Tampieri (1987), following the work of Nanni and Tampieri (1985), uses to obtain an estimate of θ_{crit}. However, a further estimate of θ_{crit} is derived here for two reasons. The first reason is that, as argued below, an improved estimate of θ_{crit} can be obtained by recognising that close to separation, non-linear terms are important and that where possible, these terms should be retained but, in the absence of any non-linear analysis, evaluated using linear results. The second is that Tampieri bases his estimate on the linear analysis of Jackson and Hunt (1975) which has been superseded by the more complete analysis of Belcher (1990). The latter analysis provides a better description of the dynamics of the flow perturbations.

Tampieri (1987) and Nanni and Tampieri (1985) work in two-dimensions and recognise separation as the occurrence of zero surface stress somewhere on the surface of the hill. They then apply a linear estimate of the perturbation surface stress and look for where the sum of this and the upstream surface stress vanishes. Close to the hill's surface, the turbulence is in local equilibrium (e.g. Belcher *et al.*, 1993). This allows the use of a first order, mixing-length turbulence closure and so

$$\tau(Z) \propto \left|\frac{\partial U}{\partial Z}\right| \frac{\partial U}{\partial Z},$$

where τ denotes the stress. Writing U as the sum of its upstream value, U_0, and the perturbation, ΔU, this expression becomes

$$\tau(Z) \propto \left|\frac{\partial U_0}{\partial Z} + \frac{\partial \Delta U}{\partial Z}\right| \left(\frac{\partial U_0}{\partial Z} + \frac{\partial \Delta U}{\partial Z}\right). \tag{1}$$

For $\partial U/\partial Z \geq 0$, as considered here, the modulus signs may be neglected and the requirement for the surface stress to vanish is that

$$\frac{\partial U_0}{\partial Z} + \frac{\partial \Delta U}{\partial Z} = 0 \quad \text{as} \quad Z \to Z_s, \tag{2}$$

where Z_s is the height of the hill's surface. The no-slip surface boundary condition gives $U_0 + \Delta U = 0$ on $Z = Z_s$, so Equation (2) requires that $\Delta U = -U_0$ close to the surface. It is this requirement that leads to a prediction of θ_{crit} as will be described in more detail later.

Nanni and Tampieri (1985) and Tampieri (1987), however, write Equation (1) in terms of the upstream stress, τ_0, and the perturbation from this, $\Delta\tau$, so that

$$\tau(Z) = \tau_0 + \Delta\tau.$$

Rather than retaining the full non-linear expression for τ in terms of the mean velocity, they subtract $\tau_0 \propto (\partial U_0/\partial Z)^2$ from Equation (1) and retain only first-order terms in ΔU to obtain:

$$\Delta\tau \propto 2\frac{\partial \Delta U}{\partial Z}\frac{\partial U_0}{\partial Z}.$$

The vanishing of τ at the surface then requires that

$$\frac{\partial U_0}{\partial Z} + 2\frac{\partial \Delta U}{\partial Z} = 0 \quad \text{as} \quad Z \to Z_s$$

or that $\Delta U = -\frac{1}{2}U_0$ close to the surface. Since the linear form for ΔU varies as θ, the peak slope of the hill, the resulting estimate of θ_{crit} is a factor of a half too small due to the neglect of the non-linear term, $(\partial \Delta U/\partial Z)^2$. Whilst at slopes such that this term is important, the linear estimate for it will be in error, it is hoped that this error will be less than that due to neglecting it completely and so here $\Delta U = -U_0$ is considered a better indication of the onset of separation. Some empirical evidence to support this, based on the resulting predictions for θ_{crit}, is given in Section 4.

In what follows, Belcher's linear analysis is used to determine the lowest slope for which

$$U_0(\hat{Z}) + \Delta U(x, \hat{Z}) \leq 0$$

for some value of x and for $\hat{Z}$ close to zero, where $\hat{Z}$ is the height above the local surface (i.e. $\hat{Z} = Z - Z_s$). This expression can be written as

$$U_0(\hat{Z})\left(1 + \frac{\Delta U(x, \hat{Z})}{U_0(\hat{Z})}\right) \leq 0. \tag{3}$$

Since $U_0(\hat{Z})$ may be assumed to be positive, Equation (3) requires that

$$\Delta S(x, \hat{Z}) \equiv \frac{\Delta U(x, \hat{Z})}{U_0(\hat{Z})} \leq -1 \tag{4}$$

where $\Delta S(x, \hat{Z})$ is the fractional speed-up factor (e.g. Jackson and Hunt, 1975). This condition will first be satisfied where $\Delta S(x, \hat{Z})$ attains its minimum value. Since only the linear perturbations are being considered, then for the sinusoidal shape considered here, this will be the negative of its maximum value which will occur near the crest of the hill. Here the small phase shift of the maximum in the velocity perturbation away from the crest ($x = 0$) is neglected so that the maximum value of $\Delta S(x, \hat{Z})$, as x is varied, can be approximated by $\Delta S(x = 0, \hat{Z}) \equiv \Delta S(\hat{Z})$, say. The linear theory of Belcher (1990) predicts that $\Delta S(\hat{Z})$ is constant through the depth of the inner surface layer and is equal to its maximum value, $\Delta S^{\max}$. Thus, Equation (4) reduces to the requirement that

$$\Delta S^{\max} \geq 1. \tag{5}$$

For hills of a general shape, this result is only an approximation. For a given shape though, it may be possible to obtain a more accurate estimate of θ_{crit} by evaluating the minimum value of $\Delta U(x, \hat{Z})$ directly from application of Fourier transforms and a linearised model of flow over hills. Here, however, we seek a more easily applicable result and, though more approximate, propose the use of Equation (5). Further, it is clear that when ΔS^{MAX} is close to unity, non-linear effects become important since the flow perturbations are of the same magnitude as the undisturbed flow and separation must be considered likely (as noted by Taylor and Lee, 1984).

Belcher's expression for the perturbation to the mean velocity (his equations 4.31 and 4.33, Chapter 2) gives the following expression for the maximum fractional speed-up:

$$\Delta S^{\text{MAX}} \simeq \theta \frac{U_0^2(h_m)}{U_0^2(l)} \left(1 + 4.2 \frac{u_*}{\kappa U_0(l)}\right), \tag{6}$$

where the constant terms in Belcher's expression have been evaluated to give the approximate number 4.2. Here, an analytical shape function has been evaluated and combined with the ratio of the hill's height scale and horizontal scale to give the maximum slope, θ. For a sinusoid, this is exact at least within the context of the linear analysis. For a general hill, replacing the complex shape factor by the maximum slope of the hill follows from the general discussion of Jackson and Hunt (1975), Hunt and Simpson (1982), the scaling arguments of Mason (1986) and the building guidelines of the UK BRE (1989) and, as discussed earlier, gives good agreement with data over, for example, Askervein and Nyland Hill.

In Equation (6), l and h_m are height scales derived from the linear analysis. Detailed discussion of these scales is given by, for example, Belcher *et al.* (1993). l is the height scale of the inner region, the region above the hill within which linear theory suggests that the turbulence is in local equilibrium, permitting use of a mixing-length closure for the turbulence. Above this height, the turbulence

perturbations are governed by rapid distortion dynamics and, as noted above, the flow perturbations are approximately inviscid. l is estimated from the following implicit equation:

$$l\left(\frac{U_0(l)}{\kappa u_*}\right) \sim \frac{1}{2}\kappa^2\lambda. \tag{7}$$

The other height scale appearing in Equation (6) is h_m. This represents the height below which shear in the upstream profile is important to the dynamics of the perturbations to the mean flow. Above this height, the mean flow perturbations are described by both inviscid and irrotational dynamics. h_m is obtained from the following implicit equation:

$$h_m\left(\frac{U_0(h_m)}{\kappa u_*}\right)^{1/2} \sim \frac{1}{4}\lambda. \tag{8}$$

Further, a neutral, logarithmic upstream (or undisturbed) wind profile is assumed:

$$U_0(Z) = \frac{u_{*0}}{\kappa}\log\left(\frac{Z}{Z_0}\right). \tag{9}$$

Here u_{*0} is the friction velocity given by the square root of the upstream surface stress, τ_0; κ is von Karman's constant; and Z_0 is the surface roughness length.

The requirement given by Equation (5), together with Equation (6), is then used to obtain the following linear estimate for θ_{crit}:

$$\theta_{\text{crit}} \simeq \left[\frac{U_0^2(h_m)}{U_0^2(l)}\left(1 + 4.2\frac{u_*}{\kappa U_0(l)}\right)\right]^{-1} \tag{10}$$

or, substituting for the assumed logarithmic, upstream profile:

$$\theta_{\text{crit}} \simeq \frac{(\log(l/Z_0))^2}{(\log(h_m/Z_0))^2(1 + 4.2/\log(l/Z_0))}. \tag{11}$$

Substituting the logarithmic profile, Equation (9), into Equations (7) and (8) for l and h_m respectively, it is found that both l/Z_0 and h_m/Z_0 are functions only of λ/Z_0. Hence Equation (11) suggests that θ_{crit} is also only a function of λ/Z_0.

The complex dependency of the critical slope for separation on the exact shape of the hill has been removed in Equation (11). This is because the shape is replaced by the maximum slope, as discussed in relation to Equation (6) above. However, it is clear that the detailed shape of the hill and exact form of the upstream wind profile will have an influence on the precise value of θ_{crit}. Whilst some allowance for such effects could, in principle at least, be made within the framework presented above, they would add considerably to the complexity of the result and hence detract from its practical applicability.

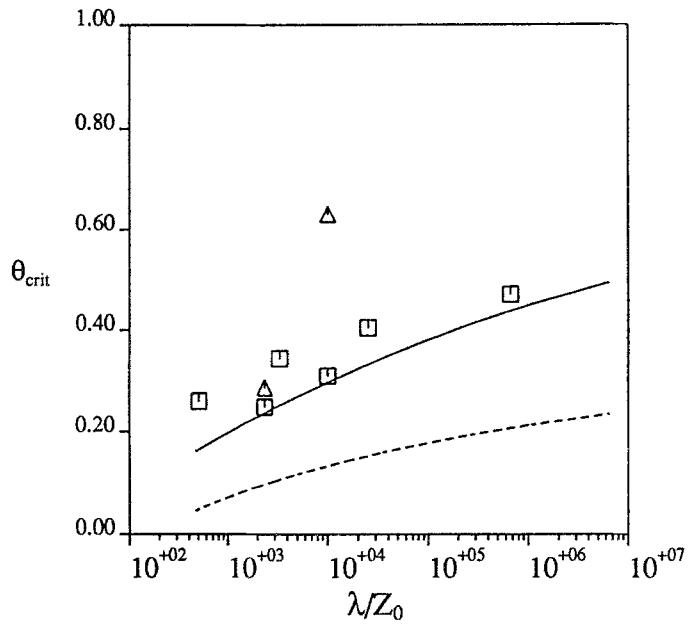

Fig. 11. The critical slope for which separation first occurs, θ_{crit}, is plotted on a linear scale against the ratio of the hill's wavelength to its surface roughness length, λ/Z_0, on a logarithmic scale. The solid line shows the predictions of θ_{crit} given by Equation (11) and the dashed line shows the predictions given by Tampieri (1987). The squares are results from two-dimensional numerical and laboratory studies. The triangles are similarly derived results but for three-dimensional hills.

Due to the various assumptions underlying its derivation, there are limitations to the shape of hills to which Equation (11) should be applied. Its predictions are likely to become inaccurate when either the hill exhibits a strong streamwise asymmetry (when the association of the maximum speed-up with the maximum slow-down will be in error) or when three-dimensional effects are likely to be important. In the latter case, the expression for the flow speed-up will still give a reasonable reflection of the adverse pressure gradient induced by the hill but the presence of lateral convergence of the flow in the lee of the hill is likely to delay the onset of separation.

4. Comparisons of the Linear Prediction of θ_{crit} with Numerical Predictions and Observations

In Figure 11, values of θ_{crit} given by Equation (11) are plotted as a solid line against λ/Z_0 on a logarithmic scale. For a fixed value of λ, as Z_0 decreases, θ_{crit} is seen to increase, in qualitative agreement with the discussion at the beginning of Section 3.

To attempt to validate the assumptions behind the derivation of Equation (11), actual values of θ_{crit} are required. Such values obtained either numerically or from

TABLE I

Values of critical slope from various studies discussed in Grant and Mason (1990) and plotted in Figure 11

Source	Critical slope	$\log_{10}(\lambda/Z_0)$	Turbulence closure
Newley (1985)	0.34	3.5	2nd order
Newley (1985)	0.40	4.4	2nd order
Taylor *et al.* (1976)	0.31	4.0	1st order
Mason and King (1984)	0.47	5.8	1st order

wind tunnel (or water channel) studies are hard to find and of course cannot be determined from field experiments unless, fortuitously the hill shows only a small separated region. A brief review of values of θ_{crit} with associated values of λ/Z_0 is given by Grant and Mason (1990) for various numerical studies of two-dimensional flows. These values are plotted in Figure 11 and are tabulated in Table I. (Where necessary it is assumed that L, the half width of the hill at half its height, is related to λ by $L \simeq \lambda/4$.) These results also include the present case for which separation is found to occur at $\theta_{\text{crit}} \simeq 0.31$ for two-dimensional hills with $\lambda/Z_0 = 10^4$.

The wind tunnel results of Gong and Ibbetson (1989) are also shown. They make measurements of turbulent flow over isolated two- and three-dimensional hills of the same shape as used in the present study. The two-dimensional hills have a peak slope of 0.25 and that of the three-dimensional hills is 0.29. In both cases, $\lambda/Z_0 \simeq 2353$. In the two-dimensional case, Gong and Ibbetson report evidence of "weakly intermittent flow separation" and for the three-dimensional case, they suggest that the flow may separate (but with different separation characteristics to the two-dimensional case, in agreement with the present findings). This suggests that in both cases, the slope is close to, though slightly greater than the critical slope. The three-dimensional case has been plotted in Figure 11 as a triangle. The present results for the three-dimensional hills suggest that separation does not occur until $\theta \simeq 0.63$ for $\lambda/Z_0 = 10^4$. This too has been plotted as a triangle.

The final results shown are those of Britter *et al.* (1981). In a wind tunnel study of turbulent flow over a two-dimensional hill, having a "Witch of Agnesi" cross-section, they report that, with $\lambda/Z_0 \simeq 508$, "separation just occurs" at $h/L = 0.4$, corresponding to a peak slope of 0.26.

4.1. Comparison with two-dimensional results

If we first consider the two-dimensional results (plotted as squares), then it is clear from Figure 11 that Equation (11) predicts the variation of θ_{crit} with λ/Z_0 quite well. As discussed above, for fixed λ, as Z_0 decreases, it becomes harder for the flow to separate. This is seen both from the line and from the model and wind

tunnel results. Equation (11) appears to be a lower bound on θ_{crit} which suggests that the non-linearity present in the full numerical models and wind tunnel flows slightly inhibits separation.

In Figure 11, the prediction of θ_{crit} given by Tampieri (1987) is also shown, plotted as a dashed line. It is seen to lie below that given by Equation (11) and is consistent with its underpredicting θ_{crit} by a factor of about two. The somewhat poor agreement seen between Tampieri's prediction and the numerical results appears to contradict Figure 4 of Tampieri (1987). In that figure, Tampieri found seemingly good agreement between his linear prediction and the results from a numerical model. (That model is very similar to the two-dimensional version of the model reported by Wood and Mason (1993).) By comparing the discussions and the results presented in Tampieri (1987), Nanni and Tampieri (1985) and Giostra *et al.* (1989), it would seem that the numerical results (plotted as a dashed line in Figure 4 of Tampieri (1987)) have been incorrectly plotted at half the critical hill height for separation whereas the other results including the linear prediction have been plotted at the full (i.e. peak-trough) hill height. Hence, the apparent agreement between the numerical results and the linear prediction of Tampieri (1987) is spurious, the latter in fact underpredicting the numerical results by a factor close to two.

4.2. Comparison with three-dimensional results

The two three-dimensional cases, plotted as triangles in Figure 11, are now considered. The upper one is the result from the present study, which appears not to separate until $h > 150$ m. The other triangle is the wind tunnel result of Gong and Ibbetson. With only two data points, it is difficult to conclude very much. Further, Gong and Ibbetson's result is only for intermittent separation which may be due to fluctuating large eddies and not representative of mean flow separation as discussed here.

The present model results suggest a larger critical slope for the three-dimensional hills than for their two-dimensional counterparts. This is in agreement with the results of Mason and Sykes (1979a and 1979b) who find that three-dimensional hills separate at a greater slope than two-dimensional ones. Their results are for laminar flows for which no closure assumptions are required.

From the model output, the maximum tangential surface pressure gradient can be evaluated. For hill heights below that for which separation occurs, this maximum pressure gradient is found to increase approximately linearly with slope. Further, for the two-dimensional hills, the rate of increase of this pressure gradient with slope is approximately 20% larger than for the three-dimensional hills. Therefore, for a given slope, two-dimensional hills have a larger adverse pressure gradient than the three-dimensional ones. Thus the three-dimensional hills may be expected to separate at a slope approximately 20% greater than the two-dimensional ones, at least for the shape of hills considered here. This would suggest that separation

over the three-dimensional hills may occur nearer to h = 150 m (θ_{crit} = 0.47) than to the plotted value of h = 200 m (θ_{crit} = 0.63). Due to the limited number of simulations performed, this latter value is the lowest value of h for which it is certain that separation occurs. Thus, the actual increase in the value of θ_{crit} from two- to three-dimensional models may be overestimated in Figure 11.

4.3. Comparisons with Atmospheric Observations

From the above discussions, it would appear that the naive application of linear theory to obtain Equation (11) gives reasonable agreement with the model and wind tunnel results.

It is interesting now to consider whether Equation (11) is in accord with atmospheric observations. Whilst θ_{crit} cannot usually be estimated from such observations, if Equation (11) gives a reasonable approximation to the actual critical slope, then observations of attached flow would be expected to generally lie below the line in Figure 11 whilst separated flows should generally lie above it. In Figure 12, the observed peak slopes of various hills over which observations have been made, are plotted against estimated values of λ/Z_0 on a logarithmic scale. The prediction of Equation (11) is also plotted, as a line. The observations have been plotted as letters whose corresponding details are presented in Tables II and III. (Note that it is the bottom left hand corner of each letter that corresponds to the actual data point.) To plot the characteristics of a particular hill in this way, its peak slope, its local roughness length and its horizontal length scale, λ, are all required. Invariably not all of these parameters are given in the literature and so some of them have to be estimated either from other parameters or from graphs. Where this has been done, the figures used are prefixed by a '$\sim$' in Table III. A further source of error is that separation may also be related to small areas of large slopes whilst the peak slopes given here are necessarily the slopes appropriate to large scales and are obtained from data which will have been implicitly, or even explicitly, smoothed.

The first thing to note from Figure 12 is that all the experiments for which separation is reported, lie above the line given by Equation (11). This agrees with the comment above that this equation provides a lower bound for θ_{crit} and also the suggestion that three-dimensional hills may have a slightly larger θ_{crit} than that predicted by Equation (11). Kettles Hill lies well below the line in agreement with its non-separated flow. Brent Knoll lies just on the line and Askervein just above it. In Table III both of these are shown to be non-separating. However, for Brent Knoll, Mason and Sykes (1979c) report fluctuations in the flow that are large enough to reverse the flow in the lee of the hill and for Askervein, Teunissen *et al.* (1987) report that quite extensive areas of separation occur in the lee of the hill for wind directions perpendicular to the hill's major axis, though this is not evident from the published data. Clearly these two cases are marginal and so are not in great disagreement with Equation (11). Thus, Equation (11) would appear to give a reasonable guideline for the onset of separation.

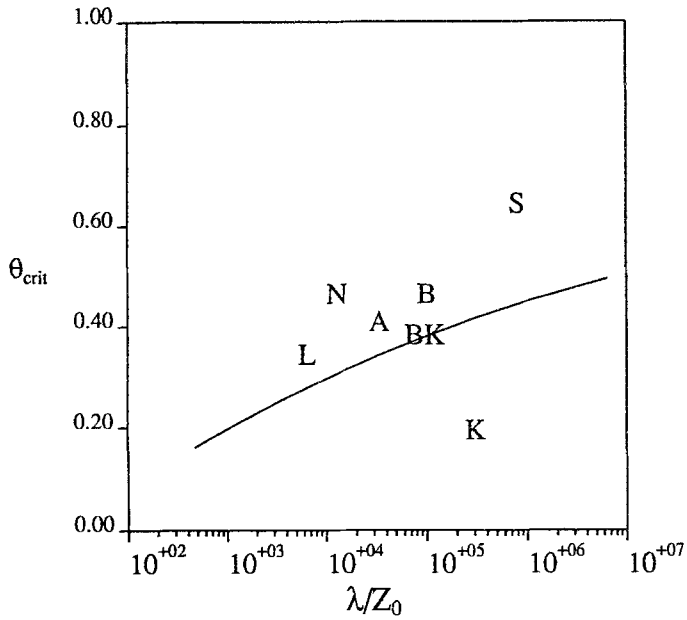

Fig. 12. Estimates of the maximum slope, θ, of various hills at which observational experiments have been carried out are plotted on a linear scale against λ/Z_0 on a logarithmic scale. The key to the symbols is given in Table II and whether the flow was observed to separate or not is indicated in Table III. Also shown are the predictions, given by Equation (11), of the critical value of slope at which separation first occurs, θ_{crit}.

TABLE II

Key to symbols plotted in Figure 12 with references

Plotted symbol	Hill	Reference(s)
A	Askervein	Taylor and Teunissen (1987)
		Salmon *et al.* (1988a)
B	Blashaval	Mason and King (1985)
BK	Brent Knoll	Mason and Sykes (1979c)
K	Kettles Hill	Salmon *et al.* (1988b)
L	Llanthony	Grant and Mason (1990)
N	Nyland	Mason (1986)
S	Sirhowy	Mason and King (1984)

5. Conclusions

The numerical simulations of neutral, turbulent flow over two- and three-dimensional hills, presented by Wood and Mason (1993), have been considered in detail to determine what is the lowest value of θ, the maximum slope of the hill,

TABLE III
Relevant details of hills plotted in Figure 12

Hill	Peak slope	Z_0 (m)	λ (m)	Separation? (Y/N)
Askervein	~0.39	0.03	800	N
Blashaval	~0.45	0.01	~800	Y
Brent Knoll	~0.36	0.02	~1200	N
Kettles Hill	~0.18	0.01	2400	N
Llanthony	~0.32	0.5	2620	Y
Nyland	0.45	0.05	~500	Y
Sirhowy	0.62	0.003	~2000	Y

required for these flows to separate. A combination of streamline plots, surface stress patterns and particle trajectory analysis has been used to visualise the flow and hence determine the onset and nature of separation.

The two-dimensional flows studied here, with $\lambda/Z_0 = 10^4$, are found to separate at $\theta = 0.31$ ($A/S_h = 0.1$). Both the packed and isolated three-dimensional cases (again with $\lambda/Z_0 = 10^4$) separate close to $\theta \simeq 0.63$ ($A/S_h \simeq 0.1$). The three-dimensional isolated hills, for which separation has just occurred, have a complex surface stress pattern, having two nodal singularities and two saddle point singularities in the lee of the hill. At the steepest slope (not presented here), for which $\theta = 0.94$ ($A/S_h \simeq 0.15$), upstream separation occurs. For the packed three-dimensional hills, the surface stress patterns are much simpler, having just one nodal and one saddle point singularity. For both three-dimensional cases the separation region is much smaller and shallower than in the two-dimensional case.

By extrapolating results of a two-dimensional linear analysis beyond its range of validity and assuming a logarithmic upstream or undisturbed velocity profile, an approximate expression for the value of θ_{crit}, the slope for which the flow first separates, is obtained:

$$\theta_{\text{crit}} \simeq \frac{(\log(l/Z_0))^2}{(\log(h_m/Z_0))^2(1 + 4.2/\log(l/Z_0))}.$$

This shows good agreement with two-dimensional numerical model predictions of θ_{crit} and is generally in accord with observations though it is suggested that this estimate represents a lower bound to the actual critical slope for separation. Due to the approximations made in deriving this estimate for θ_{crit}, it is likely to become less accurate for hills with a strong streamwise asymmetry.

The only other known estimate for θ_{crit} is that given by Tampieri (1987) which is approximately half that suggested here. This is because the present derivation retains a term which is non-linear in the flow perturbation, ΔU, and estimates this

non-linear term using linear results. Though this approach is not strictly rigorous, the comparisons with numerical and experimental results, as well as with atmospheric observations, suggest that it gives better results than completely neglecting this term, as Tampieri did.

Finally, as well as providing a useful, practical estimate of when flow over a hill is likely to separate, the expression for θ_{crit} gives a method of predicting those hills for which linear analysis is likely to be useful. This can be achieved by comparing the actual maximum slope of a particular hill, θ, with the corresponding prediction of θ_{crit}. Thus, for $\theta/\theta_{\text{crit}} < 1$, it is expected that linear theory would provide useful guidance on the flow structure whilst for $\theta/\theta_{\text{crit}} \gtrsim 1$, it is unlikely to do so.

Acknowledgements

I would like to thank Paul Mason and Alan Ibbetson for their help and support during the period of this work and Alan Grant, Fiona Hewer and David Pick who provided helpful comments on this manuscript.

References

Belcher, S. E.: 1990, *Turbulent Boundary Layer Flow over Undulating Surfaces*, Ph.D. dissertation, Cambridge University.

Belcher, S. E., Newley, T. M. J., and Hunt, J. C. R.: 1993, 'The Drag on an Undulating Surface Due to the Flow of a Turbulent Boundary Layer', *J. Fluid Mech.* **249**, 557–596.

BRE: 1989, *The Assessment of Wind Speed over Topography*, Building Research Establishment, Digest 346, HMSO, London.

Britter, R. E., Hunt, J. C. R., and Richards, K. J.: 1981, 'Air Flow over a Two-Dimensional Hill: Studies of Velocity Speed-Up, Roughness Effects and Turbulence', *Quart. J. Roy. Meteorol. Soc.* **107**, 91–110.

Clark, T. L.: 1977. 'A Small-Scale Dynamic Model using a Terrain-Following Transformation', *J. Comput. Phys.* **24**, 186–215.

Giostra, U., Tampieri, F., and Trombetti, F.: 1989, 'On the Onset of Separation in Turbulent Boundary Layer Flow over Two-Dimensional Humps of Various Size', *Nuovo Cimento*, **12C**, 649–661.

Grant, A. L. M. and Mason, P. J.: 1990, 'Observations of Boundary-Layer Structure over Complex Terrain', *Quart. J. Roy. Meteorol. Soc.* **116**, 159–186.

Gong, W. and Ibbetson, A.: 1989, 'A Wind Tunnel Study of Turbulent Flow over Model Hills', *Boundary-Layer Meteorol.* **49**, 113–148.

Hunt, J. C. R., Abell, C. J., Peterka, J. A., and Woo, H.: 1978, 'Kinematical Studies of Flow Around Free or Surface-Mounted Obstacles; Applying Topology to Flow Visualisation', *J. Fluid Mech.* **86**, 179–200.

Hunt, J. C. R., Leibovich, S., and Richards, K. J.: 1988, 'Turbulent Shear Flows over Low Hills', *Quart. J. Roy. Meteorol. Soc.* **114**, 1435–1470.

Hunt, J. C. R. and Simpson, J. E.: 1982, 'Atmospheric Boundary Layers over Non-Homogeneous Terrain', in E. J. Plate (ed.), *Engineering Meteorology*, Chapter 7, Elsevier Sci., Amsterdam, pp. 269-318.

Jackson, P. S. and Hunt, J. C. R.: 1975, 'Turbulent Wind Flow over a Low Hill', *Quart. J. Roy. Meteorol. Soc.* **101**, 929–955.

Lighthill, J.: 1989, *An Informal Introduction to Theoretical Fluid Mechanics*, Oxford, Clarendon Press, 260 pp.

Mason, P. J.: 1986, 'Flow over the Summit of an Isolated Hill', *Boundary-Layer Meteorol.* **37**, 385–405.

Mason, P. J. and King, J. C.: 1984, 'Atmospheric Flow over a Succession of Nearly Two-Dimensional Ridges and Valleys', *Quart. J. Roy. Meteorol. Soc.* **110**, 821–845.

Mason, P. J. and King, J. C.: 1985, 'Measurements and Predictions of Flow and Turbulence over an Isolated Hill of Moderate Slope', *Quart. J. Roy. Meteorol. Soc.* **111**, 617–640.

Mason, P. J. and Sykes, R. I.: 1979a, 'Three-Dimensional Numerical Integrations of the Navier–Stokes Equations for Flow over Surface-Mounted Obstacles', *J. Fluid Mech.* **91**, 433–450.

Mason, P. J. and Sykes, R. I.: 1979b, 'Separation Effects in Ekman Layer Flow over Ridges', *Quart. J. Roy. Meteorol. Soc.* **105**, 129–146.

Mason, P. J. and Sykes, R. I.: 1979c, 'Flow over an Isolated Hill of Moderate Slope', *Quart. J. Roy. Meteorol. Soc.* **105**, 383–395.

Nanni, S. C. and Tampieri, F.: 1985, 'A Linear Investigation on Separation in Laminar and Turbulent Boundary Layers over Low Hills and Valleys', *Nuovo Cimento* **8C**, 579–601.

Newley, T. J.: 1985, *Turbulent Airflow over Hills*, Ph.D. dissertation, Cambridge University.

Salmon, J. R., Bowen, A. J., Hoff, A. M., Johnson, R., Mickle, R. E., Taylor, P. A., Tetzlaff, G., and Walmsley, J. L.: 1988a, 'The Askervein Hill Project: Mean Wind Variations at Fixed Heights Above Ground', *Boundary-Layer Meteorol.* **43**, 247–271.

Salmon, J. R., Teunissen, H. W., Mickle, R. E., and Taylor, P. A.: 1988b, 'The Kettles Hill Project: Field Observations, Wind-Tunnel Simulations and Numerical Model Predictions for Flow over a Low Hill', *Boundary-Layer Meteorol.* **43**, 309–343.

Tampieri, F.: 1987, 'Separation Features of Boundary-Layer Flow over Valleys', *Boundary-Layer Meteorol.* **40**, 295–307.

Taylor, P. A., Gent, P. R., and Keen, J. M.: 1976, 'Some Numerical Solutions for Turbulent Boundary Layer Flow above Fixed, Rough, Wavy Surfaces', *Geophys. J. R. Astr. Soc.* **44**, 177–201.

Taylor, P. A. and Lee, R. J.: 1984, 'Simple Guidelines for Estimating Wind Speed Variations due to Small Scale Topographic Features', *Climatol. Bulletin* **18**, 3–32.

Taylor, P. A. and Teunissen, H. W.: 1987, 'The Askervein Hill Project: Overview and Background Data', *Boundary-Layer Meteorol.* **39**, 15–39.

Teunissen, H. W., Shokr, M. E., Bowen, A. J., Wood, C. J., and Green, D. W. R.: 1987, 'The Askervein Hill Project: Wind-Tunnel Simulations at Three Length Scales', *Boundary-Layer Meteorol.* **40**, 1–29.

Van Dommelen, L. L. and Cowley, S. J.: 1990, 'On the Lagrangian Description of Unsteady Boundary-Layer Separation. Part 1. General Theory', *J. Fluid Mech.* **210**, 593–626.

Wood, N.: 1992, *Turbulent Flow over Three-Dimensional Hills*, Ph.D. thesis. University of Reading.

Wood, N. and Mason, P. J .: 1993, 'The Pressure Force Induced by Neutral Turbulent Flow over Hills', *Quart. J. Roy. Meteorol. Soc.* **119**, 1233–1267.